Okhotsk Sea and Polar Oceans Research 6 (2022) 36-41

Article

Snowfall detection by a newly deployed X-band Doppler radar at Syowa Station, Antarctica

Naohiko HIRASAWA[1,2], Hiroyuki KONISHI[3], Yasushi FUJIYOSHI[4], Kazuhiro SHIBATA[1] and Katsushi IWAMOTO[5]

[1] *National Institute of Polar Research, Tachikawa, Tokyo, Japan*
[2] *Department of Polar Science, School of Multidisciplinary Sciences, SOKENDAI (The Graduate University for Advanced Studies), Tachikawa, Tokyo, Japan*
[3] *Division of Math, Sciences, and Information Technology in Education, Osaka-kyoiku University, Osaka, Japan*
[4] *Emeritus Prof., Hokkaido University, Sapporo, Hokkaido, Japan*
[5] *Fisheries Research Division, City of Mombetsu, Mombetsu, Hokkaido, Japan*

(Received November 4, 2021; Revised manuscript accepted December 28, 2021)

Abstract

As part of the 62nd Japanese Antarctic Research Expedition (JARE), we deployed an X-band Doppler radar at Syowa Station in February 2021 to study various types of snowfall events. The tentative results of the snowfall detectability experiments show that this radar system can observe heavy snowfall events during periods of strong wind caused by synoptic-scale disturbances. In addition, by combining the data from this radar with those of a previously installed ceilometer and disdrometer, we will be able to observe almost all snowfall events at Syowa Station.

Keywords: Antarctic snowfall, X-band Doppler radar, Syowa Station, JARE

1. Introduction

Changes in the mass of the Antarctic ice sheet are a major concern in studies on global warming. The IPCC (Intergovernmental Panel on Climate Change) Special Report (Meredith *et al.* 2019; The IMBIE (Ice sheet Mass Balance Inter-comparison Exercise) Team 2018) states that while the mass of the entire Antarctic ice sheet has been decreasing since the 1990s, the mass of the ice sheets in the western region of East Antarctica, which includes the Japanese sphere of activities, has increased from the mid-2000s to the present.

The mass of the Antarctic ice sheet increases due to snowfall and decreases due to coastal iceberg runoff and melting. In order to accurately forecast changes in the mass of the Antarctic ice sheet, being able to accurately measure the amount of snowfall is becoming increasingly important. However, the absence of any long-term precipitation observations in Antarctica makes it difficult to directly examine the relationship between global warming and climate change.

Measuring precipitation with high reliability is still challenging, especially in Antarctica where strong winds decrease the catch rate of snow particles by snow gauges (WMO 2018). For example, Hirasawa *et al.* (2018) reported that a gauge-type instrument, RT3 (the primary instrument used to measure snowfall by the Japan Meteorological Agency (JMA)), underestimated the total snowfall amounts by up to 60%. Heavy precipitation events associated with synoptic-scale disturbances are often accompanied by blizzards. Based on estimates by the climate model RACMO2 (Lenaerts *et al.* 2013; Marshall *et al.* 2017), Turner *et al.* (2019) showed that the most extreme precipitation events (i.e., events with precipitation intensities in the top 10%) are responsible for approximately 50% of the annual precipitation in Antarctica. It is therefore crucially important to be able to measure snowfall amounts under the strong wind conditions that are associated with synoptic-scale disturbances.

Under strong wind conditions, snow particles are liberated from the snow surface and are resuspended in the atmosphere. As a result, measurements inevitably contain a mixture of normal snowfall and such drifting snow. Although the proportion of drifting snow is relatively higher near the surface (*e.g.*, Kobayashi 1978; Takahashi 1985; Mann *et al.* 2000; Nishimura and Nemoto 2005), it can reach heights of up to 1000 m above the Antarctic ice sheet (Palm *et al.* 2011). Since observing drifting snow directly is difficult, the mixing of drifting snow and snowfall need to be considered in order to obtain an accurate picture of snowfall.

The second reason why measuring precipitation with high reliability in Antarctica is difficult is because the snowfalls in Antarctica are extremely weak and occur over a long period. Especially in inland areas, such weak snowfalls (also referred to as clear sky precipitation or diamond dust) occur during about 80% of the year (*e.g.*, Kuhn *et al.* 1975; Schwerdtfeger 1984;

King and Turner 1997). For example, at Dome Fuji, the annual snowfall accumulation is approximately 30 mm; if half of that, 15 mm, is due to the weak snowfalls that occur over 292 days (80% of 365 days), then the daily snowfall amount is about 0.05 mm (approximately 0.0003 mm/min.). Since measuring such weak snowfall by mass is impractical, another method is required.

Over the last decade, estimates of snowfall have been conducted at several stations in Antarctica, either by direct mass observations or by remote sensors, such as lidar and radar (Fig. 1). For example, an X-band polarimetric radar, a micro rain radar, a weighing gauge, and a multi-angle snowflake camera have been used for this purpose at the French Dumont d'Urville Station since November 2015 (Grazioli *et al.* 2017). Micro rain radars have also been installed at the Belgian Princess Elisabeth Station (Duran-Alarcon *et al.* 2019) and the Italian Mario Zucchelli Station (Souverijns *et al.* 2018). Intercomparison studies of data collected at these stations and satellite and climate reanalysis data have been undertaken. At Syowa Station, X-band radar observations have been conducted from 1989 to 1990. The findings of that project showed that precipitation occurred on 130 days per year, the total precipitation amount was about 200 mm per year, and the frequency of precipitation events appeared to be higher in spring and autumn (Konishi and Endo 1997; Konishi *et al.* 1998).

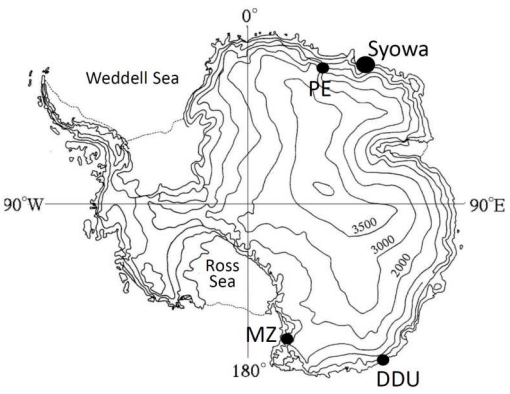

Fig. 1 Locations of Syowa and other Antarctic stations where micro rain radar systems have been deployed. PE: Princess Elisabeth Station, DDU: Dumont d'Urville Station, MZ: Mario Zucchelli station.

Since March 2021, a new project by the 62nd Japanese Antarctic Research Expedition, JARE-62) was initiated at Syowa Station. The project involved deploying a new X-band (9.4 GHz) radar and a ceilometer, which are being operated in conjunction with a disdrometer that was installed previously. The main aims of the project are to measure the annual snowfall amount, including snowfalls during strong winds, and very weak snowfall. The X-band radar can also obtain the Doppler velocity and Doppler spectrum width at high temporal (several seconds) and spatial (several meters) resolutions. Therefore, when combined with the atmospheric radar, PANSY (Program of the Antarctic Syowa MST/IS Radar) (Sato *et al.* 2014), this radar will be able to accurately clarify the atmospheric structure and conditions (wind speed and turbulence) under blizzard conditions. Furthermore, in response to the Special Observation Period (SOP) of the Year of Polar Prediction in the Southern Hemisphere (YOPP-SH) (Bromwich *et al.* 2020), which is planned for April to July 2022, the accuracy of the numerical weather prediction models will be verified with the obtained datasets.

From the observations conducted to date (approx. 6 months), snowfall intensity and Doppler velocity have been observed within a range of 2-3 km around the radar site during strong winds associated with synoptic-scale disturbances (Hirasawa *et al.* 2021). However, shallow snow clouds composed of small ice particles were not observed due to their low backscattering intensity. This project aims to capture all of the snowfall at Syowa Station using a combination of the radar, the ceilometer, and the disdrometer. Therefore, this study will examine the detection of snowfall by this radar at Syowa Station.

2. Syowa Station and observations

2.1 X-band Doppler radar

Syowa Station (39°35'E, 69°00'S) is located on East Ongul Island, approximately 4 km off the coast of the Antarctic ice sheet (Figs. 1 and 2a). The station faces a bay (Lutzow-Holm Bay) that cuts to the south, and the coast runs north-south. The katabatic wind that descends on the slope of the ice sheet reflects the terrain and blows from the northeast of Syowa Station; this wind is the prevailing wind at Syowa Station. When a relatively strong northerly wind is associated with synoptic-scale disturbances, the orographic blocking of the ice sheet generates a low-level jet along the coast, which is also a northeasterly wind (Yamada and Hirasawa 2018).

The radar, manufactured by JRC Ltd., Japan, was setup within a radome on a hill at an elevation of 21 m above sea level (asl) (Fig. 2b). The antenna rotates vertically 50° to the east of north. The continental coast is within a radius of 10 km (Fig. 2a).

The transmission frequency of the radar is 9.4 GHz. The azimuth sampling interval is about 0.33°, and the sampling interval is about 3.75 m. The rotation speed is 24 rpm. These attributes mean that the system is capable of detecting fast-moving and fine structures within snowfall fields.

2.2 Other measurements

A ceilometer (CT25K, Vaisala, Finland) and a disdrometer (LPM, Thies Clima, Germany) are used to

cross-check the radar data and to capture weak snowfall phenomena. The surface wind speed data are obtained from the JMA website.

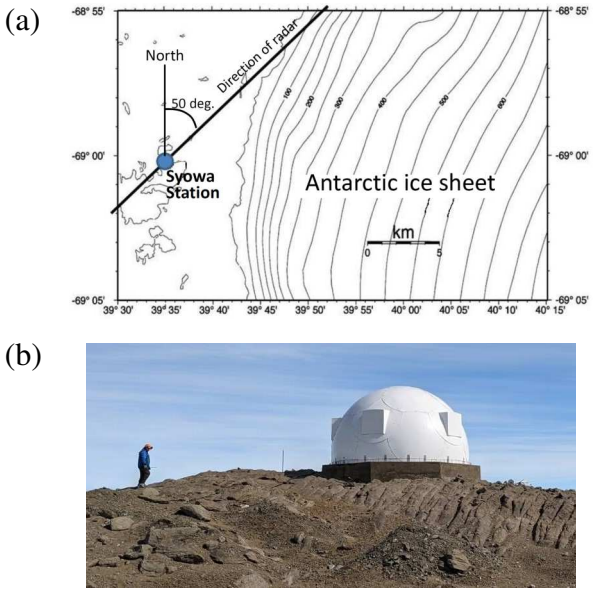

Fig. 2 Scanning direction of the X-band Doppler radar (a), and a picture of the radome (b).

3. Radar reflection intensity (RRI)

3.1 Overview of the RRI

The radar equation for this system is:

$$10\log Z = \frac{(X(L) - 32768)}{100} + 40\log L + \alpha \quad (1),$$

where 10log$Z$ is the backscattering coefficient for the radio waves, X(L) is the signal of the received electric power from distance L. α is a constant that is specific to the instrument, but which has not yet been determined.

The first term on the right side of the equation indicates the received electric power (10logPr) from a distance L. The second term is for correction of the distance. In this paper, the first and second terms are applied, and the distance-corrected 10logPr (referred to as radar reflection intensity: RRI) is used for the analysis.

3.2 Characteristics of the RRI for a typical snowfall event

Figure 3 shows a vertical section of the RRI at 18LT, 24 October 2021. The RRI is discontinuous around 2 km because the observation specifications differ for areas within and beyond a 2 km radius. Although the radar echoes are less intense within a 2 km radius, relatively intense radar echoes appear at 500 to 1500 m just above the radar site (r=0). This relatively intense layer connects to one outside the 2 km radius (on the right-hand side of the panel).

It is preferable to use the RRI near the surface to evaluate the snowfall intensity. However, the radar echo within a radius of 300 m is noisy. Therefore, we set a reference area for the RRIs at 400 m to 600 m, as shown by a rectangle above the radar in Fig. 3.

3.3 Determining the threshold of the RRI for the reference area for detecting snowfall

We calculated the deviation in the average RRI in the reference area (RRI-index). Figure 4a shows the temporal change in the RRI-index at 3-hour intervals in October 2021. The RRI-index is typically around 0.1 and lower than 0.2. The radar image shown in Fig. 3 is the top sixth highest value of the RRI-index (12.9) in the period.

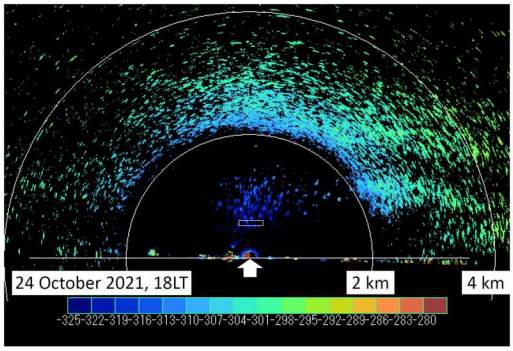

Fig. 3 A vertical section of the RRI during a snowfall event at 18LT, 24 October 2021. The RRI-index values are shown by the color bar below the vertical section. The bold white arrow at center bottom indicates the location of the radar. The white rectangle shows the approximate area used to evaluate the snowfall intensity using RRI-index values.

Figure 4b shows temporal changes in precipitation intensity (mm/hr) measured by LPM. Comparing Fig. 4a with Fig. 4b, heavy precipitation events on 7, 23, 24, 25, 28, 29, and 30 October were detected by the X-band radar. However, the RRI-index values ranged from 0 to 0.2, even when the LPM did not detect any precipitation.

The scatter plot in Fig. 5 clearly shows the relationship between the RRI-index and the precipitation intensity. Green circles indicate RRI-index values greater than 1, which is when high-intensity precipitation events occurred. A positive correlation was observed between the RRI-index and the precipitation intensity, but the degree of the scatter was not small, likely due to the low-level sublimation of snowfall particles (*e.g.*, Grazioli *et al.*, 2017) and the mixture of the drifting snow.

On the other hand, some plots had RRI-index values of 0.2-1.0 and precipitation intensities of about 0.01 mm/hr or less, indicating that the radar was capable of detecting weak precipitation in some cases; these findings are discussed in the next section.

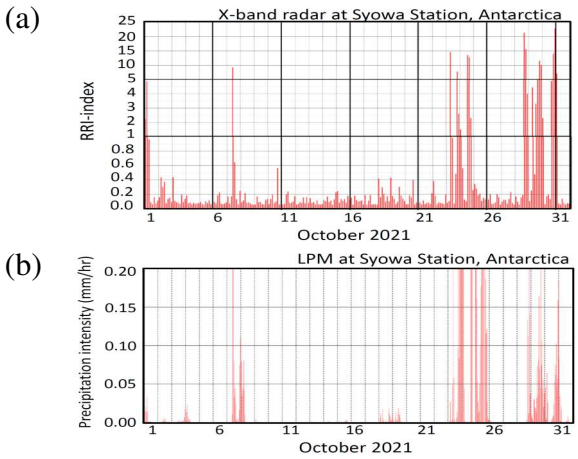

Fig. 4 (a) Time series of the RRI-index at 3-hour intervals for October 2021. Note that the intervals on the vertical axis are different at the top, middle, and bottom. (b) Time series of precipitation intensity (mm/hr) in October 2021 measured by LPM.

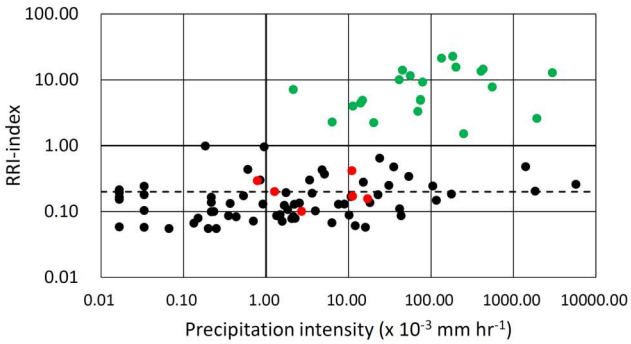

Fig. 5 Scatter plot of precipitation intensity measured by LPM and RRI-index values in October 2021. Green circles indicate RRI-index values greater than 1, which is when high-intensity precipitation events occurred. Red circles for 18 October indicate precipitation events of lower intensity.

4. Threshold performance

4.1 Weak snowfall events

As stated above, an RRI-index value of 0.2 could potentially be used as a threshold for identifying weak snowfall events. Here, we discuss the possibility of using this threshold for weak snowfall events.

Figure 6a shows a time series of RRI-index values from 17 to 19 October. Values greater than 0.2 appear at 03 and 09LST on 18 October and at 00 and 15LST on 19 October. On the other hand, the disdrometer, LPM, detected weak snowfall from 03LST on 18 October to 15LST on 19 October (Fig. 6b). Figure 6c shows a time-height cross-section of the backscatter coefficient for the ceilometer, CT25K, on 18 October 2021. The higher backscattering ratios below 1 km at 03, 06, 18LT indicate snowfall, corroborating findings obtained by the disdrometer. However, the six red circles in Fig. 5 does not indicate clear correlation between the RRI-index and the LPM precipitation intensity. Therefore, determining an appropriate relationship between the RRI-index and the LPM precipitation intensity will require additional examination.

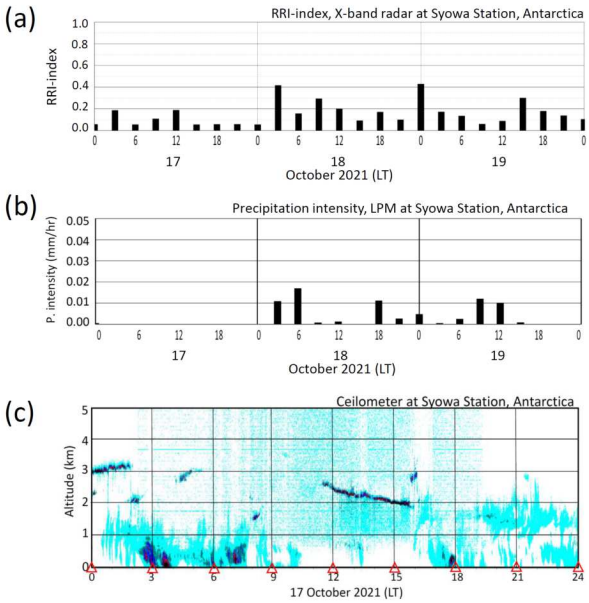

Fig. 6 Time series of RRI-index values derived from (a) the radar, (b) precipitation intensity (mm/s) from the disdrometer, LPM, for 17-19 October 2021, and (c) time-height section of backscatter coefficient measured by the ceilometer, CT25K on 18 October 2021.

4.2 A strong wind event

A synoptic-scale disturbance occurred over Syowa Station from 23 to 25 October, causing strong winds and relatively heavy snowfall, as shown in Figs. 5 and 7.

Here, we focus on the 25 October event. The surface wind speed throughout the day was higher than 15 m/s. The RRI-index values were greater than 10 on 24 October, but decreased to a maximum of around 0.2 during the day (Fig. 4). On the other hand, disdrometer measurements indicated very intense precipitation during the day (Fig. 5). Compared with the X-band radar data, we can safely conclude that most of the snowfall measured by the disdrometer was not due to precipitation particles, but due to blowing snow.

In addition, measuring snowfall with the ceilometer during such strong winds is difficult because the blowing snow causes very low visibility above the surface layer (data not shown).

Based on these findings, we conclude that the X-band radar is capable of detecting snowfall during strong wind events with relatively weak snowfall. However, we can capture weak snowfalls more

accurately by combining the radar with the ceilometer and the disdrometer.

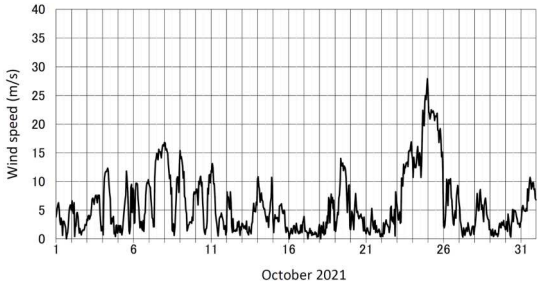

Fig. 7 Time series of surface wind speed (m/s) at Syowa Station in October 2021.

4.3 Application to more extended time series after May 2021

At Syowa Station, synoptic-scale disturbances are typically associated with strong winds exceeding 20 m/s. As the blowing snow masks snowfall, measuring the snowfall intensity and confirming the presence or absence of snowfall from the surface is difficult.

Figure 8 shows representative time series data for surface wind speed at Syowa Station, with precipitation assessed using two kinds of thresholds, i.e., RRI-index values of 1.0 and 0.2. The figure shows that the intense snowfall associated with RRI-index values greater than 1.0 does not always occur at wind speeds greater than 20 m/s, as seen in mid-July and mid-August. On the other hand, weak snowfall events with RRI-index values greater than 0.2 occurred relatively frequently throughout this period. It can therefore be inferred that the lower threshold of 0.2 is better suited to extracting some of the clear-sky precipitation events, which means that we will be able to accurately evaluate almost all snowfall events at Syowa Station throughout the year.

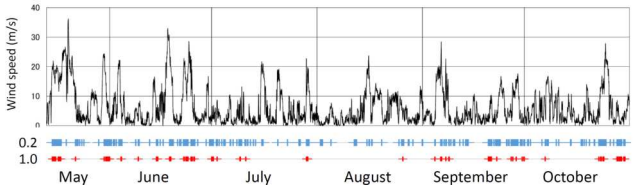

Fig. 8 Time series of surface wind speed (m/s) at Syowa Station from May to October 2021 (top panel) and detected snowfall events for RRI-index values of 0.2 (blue crosses) and 1.0 (red crosses) (bottom panel).

5. Conclusion

An X-band Doppler radar was deployed at Syowa Station in February 2021 as part of the 62nd Japanese Antarctic Research Expedition (JARE), which sought to observe snowfall and study the microphysical processes associated with precipitating cloud systems.

After gradually optimizing the radar parameters for snowfall at Syowa Station over a six-month period, the operational parameters were finalized in mid-May. Since then, we have examined the observation capabilities of the radar for investigating snowfall events at Syowa Station and have found the following:

(1) The radar was capable of observing heavy snowfall events under the most severe wind conditions that have been recorded at Syowa Station to date.

(2) The snowfall intensities during the events mentioned above were not always strong, but sometimes there was almost no snowfall.

(3) Even when the radar did not detect snowfall, the ceilometer and the disdrometer detected snowfall. Therefore, we will observe almost all snowfall events at Syowa Station by combining the data from this radar with those obtained from these instruments.

Finally, when estimating the amount of snowfall at Syowa Station with these data, we also confirmed the need to consider low-level sublimation of snowfall particles as well as the mixture of drifting snow and snowfall.

Acknowledgements

This study was conducted as part of a scientific project entitled, "Annual observation of amount of snowfall by using a precipitation radar around Syowa Station, Antarctica" (Project no. AP0934), administered by the Japanese Antarctic Research Expedition (JARE). The authors wish to thank the Institute of Low Temperature Science, Hokkaido University for providing the radar system. The authors express considerable thanks to Mr. Masahiko Takamatsu, Japan Radio Co. Ltd. (JRC) for his expert advice on starting the radar observations, and the JARE-62 members for installing the system. This study was supported by National Institute of Polar Research (NIPR) through Project Research No. KP-302.

References

Bromwich, D. H., and 37 co-authors (2020): The Year of Polar Prediction in the Southern Hemisphere (YOPP-SH), *Bull. Amer. Meteor. Soc.*, **101**(10): E1653–E1676. https://doi.org/10.1175/BAMS-D-19-0255.1.

Durán-Alarcón, C. and 7 co-authors (2019): The vertical structure of precipitation at two stations in East Antarctica derived from Micro Rain Radars. *The Cryosphere*, **3**(1), 247–264. https://doi.org/10.5194/ tc-13-247-2019

Grazioli, J. and 6 co-authors (2017): Measurements of precipitation in Dumont d'Urville,Adélie Land, East Antarctica. *The Cryosphere*, **11**(4), 1797–1811. https://doi.org/10.5194/tc-11-1797-2017

Grazioli, J., Madeleine, J.-B., Gallée, H., Forbes, R. M., Genthon, C., Krinner, G., & Berne, A. (2017): Katabatic winds diminish precipitation contribution to the Antarctic ice mass balance. PNAS, 114(41), 10858–10863. https://doi.org/10.1073/pnas.1707633114

Hirasawa, N., H. Konishi, Y. Fujiyoshi, K. Shibata and K. Iwamoto (2021): A strong snowfall event with low level jet detected by X-band Doppler radar at Syowa Station, Antarctica, under the influence of a synoptic-scale

disturbance. 2021 autumn meeting of the Meteorological Society of Japan, Proceedings, 120, 168p. (in Japanese)
Hirasawa, N., H. Konishi, K. Nishimura, C Genthon and project group of Japan Meteorological Agency (2018): SPICE site report: Rikubetsu, Japan. *WMO Solid Precipitation Intercomparison Experiment (SPICE) (2012-2015), Instruments and Observing Methods*, **131**, Annex 8.3.
King, J. C. and J. Turner (1997): Antarctic meteorology and climatology, *Atmospheric and Space Science Series*, Cambridge University Press, 409 p.
Kobayashi, S. (1978). Snow Transport by Katabatic Winds in Mizuho Camp Area, East Antarctica. J. Meteorol. Soc. Japan, Ser. II, **56**(2), 130–139. https://doi.org/10.2151/jmsj1965.56.2_130
Konishi, H. and T. Endo (1997): Characteristics and seasonal variations of precipitation phenomena at Syowa Station. *Antarctic Record*, **41**, 103-129. (in Japanese)
Konishi, H., M. Wada and T. Endoh (1998): Seasonal variations of clouds and precipitation at Syowa Station Antarctica. *Annals of Glaciology*, **27**, 597-602.
Kuhn M. H., A. J. Reordan and I. A. Wagner (1975): The climate of Plateau Station. *Climate of the Arctic*, 255-267.
Lenaerts, J., E. van Meijgaard, M. R. van den Broeke, J. M. Ligtenberg, M. Horwath and E. Isaksson (2013): Recent snowfall anomalies in Dronning Maud Land, East Antarctica, in a historical and future climate perspective. *Geophys. Res. Lett.*, **40**, 2684–2688. https://doi.org/10.1002/grl.50559
Mann, G. W., Anderson, P. S., & Mobbs, S. D. (2000). Profile measurements of blowing snow at Halley, Antarctica. Journal of Geophysical Research: Atmospheres, 105(D19), 24491–24508. https://doi.org/10.1029/2000JD900247
Marshall, G. J., D. W. J. Thompson and M. R. van den Broeke (2017): The signature of Southern Hemisphere atmospheric circulation patterns in Antarctic precipitation. *Geophys. Res. Lett.*, **44**, 11,580–11,589. https://doi.org/10.1002/2017GL075998
Meredith, M. and 12 co-authors (2019): Polar Regions, In *IPCC Special Report on the Ocean and Cryosphere in a Changing Climate* [Pörtner, H.-O. and 12 co-authors (eds.)]. In press.
Nishimura, K., & Nemoto, M. (2005): Blowing snow at Mizuho station, Antarctica. Philosophical Transactions of the Royal Society A: Mathematical, Physical and Engineering Sciences, 363(1832), 1647–1662. https://doi.org/10.1098/rsta.2005.1599
Palm, S. P., Yang, Y., Spinhirne, J. D., & Marshak, A. (2011): Satellite remote sensing of blowing snow properties over Antarctica. *J. Geophys. Res. Atmos.*, **116**(D16). https://doi.org/10.1029/2011JD015828
Sato, K., and 9 co-authors (2014): Program of the Antarctic Syowa MST/IS Radar (PANSY). *J. Atmos. Solar-Terr. Phys.*, **118**A, 2-15, doi:10.1016/j.jastp.2013.08.022.
Schwerdtfeger, W. (1984): Weather and climate of the Antarctic, *Development in atmospheric Science*, **15**, Amsterdam, Elsevier, 261 p.
Souverijns, N. and 10 co-authors (2018): Evaluation of the CloudSat surface snowfall product over Antarctica using ground-based precipitation radars. *The Cryosphere*, **12**(12), 3775–3789. https://doi.org/10.5194/ tc-12-3775-2018
Takahashi, S. (1985). Characteristics of Drifting Snow at Mizuho Station, Antarctica. Annals of Glaciology, 6, 71–75. https://doi.org/10.3189/1985AoG6-1-71-75
The IMBIE team (2018): Mass balance of the Antarctic Ice Sheet from 1992 to 2017, *Nature* **558**, 219-222. doi:10.1038/s41586-018-0179-y.
Turner, J. and 12 co-authors (2019): The dominant role of extreme precipitation events in Antarctic snowfall variability. *Geophys. Res. Lett.*, **46**, 3502–3511. https://doi.org/10.1029/2018GL081517
WMO Solid Precipitation Intercomparison Experiment (SPICE) (2012-2015), *Instruments and Observing Methods*, **131**. https://library.wmo.int/opac/
Yamada, K. and N. Hirasawa (2018): Analysis of a record breaking strong wind event at Syowa Station in January 2015, *J. Geophys. Res.*, Atmosphere, JGRD55093, DOI: 10.1029/2018JD02887

Summary in Japanese

和文要約

南極昭和基地に設置された X-band ドップラーレーダーの降雪現象の検出特性

平沢尚彦 [1,2], 小西啓之 [3], 藤吉康志 [4], 柴田和宏 [1], 岩本勉之 [5]

[1] 国立極地研究所, [2] 総合研究大学院大学, [3] 大阪教育大学, [4] 北海道大学名誉教授, [5] 北海道紋別市役所

南極氷床の質量は降雪によって涵養され，沿岸での氷山流出や融解によって消耗する．温暖化の進行に伴って南極氷床全体の質量は減少し，その水は海水準の増加に向かい始めた．今後の南極氷床の質量の変化を知るために，降雪量を精度よく把握することがますます重要になっている．しかしながら，南極域の降雪量の観測や知見が未だ不十分である．昭和基地では，第 62 次南極観測隊の中で，2021 年 2 月に X-band ドップラーレーダーを導入し，昭和基地の現在の降水量の把握や降水形成過程の解明を目指している．これまでの約半年間で昭和基地の降雪に適した観測の仕方を試行錯誤し，5 月半ばにそれを確定した．本論文では，昭和基地の降雪イベントについて，当レーダーの観測限界について考察した。以下は現時点での結論である．

①これまで昭和基地で観測ができなかった総観規模擾乱に影響された強風期間の降雪量の観測が可能である．
②上記の強風現象期間中の降雪強度は常に強いわけではなく，無降雪に近い期間がある．
③シーロメータで検出されている微弱な降雪には，当レーダーで検出できない現象がある．

これらの結果から，当レーダーとシーロメータやディスドロメータは相補的であり，これらの測器を組み合わせることで，昭和基地におけるほぼ全ての降雪イベントに対応できると考えている．

Correspondence to: Naohiko Hirasawa, hira.n@nipr.ac.jp